Chapter 2
Particle Size Classification by Fluidization

2.1 Characteristic of Fluidized Bed

A gas fluidized bed may be divided into two zones, the bubbling zone or dense phase and freeboard zone or lean phase, as shown in Figure 2.1. In the former zone, bubbles grow by coalescence and rise to the surface of bed where they break. In the latter zone, particles are thrown up, into this area after bubble break. Stratification phenomena occurred in this region, or in other word, classification and arrangement of the solids according to their size into more or less well defined zones or layers vertically oriented (Figures 2.1 and 2.2) (5). Consider a particle moving upward by a constant gas velocity, it will develop drag force during movement until the sum of drag force and buoyant force are counter-balanced with acting force, and particle will move with constant velocity, that is, terminal velocity (6). In fluidized bed, when bubbles burst at the bed surface, the particles are thrown upward with different initial velocity. This initial solid velocity distribution range from 0 to 8 times the bubble velocity at the bed surface, with the average value of 2.1 times (7). The height at which particle could reach and fall back in freeboard zone depends upon its size and density. The upper boundary where falling back of particle does not occur is called the transport disengaging height (TDH). Above this boundary, only fine particles whose superficial velocity is in excess of their terminal velocity are carried out from the system, as shown in Figure 2.3 (5).

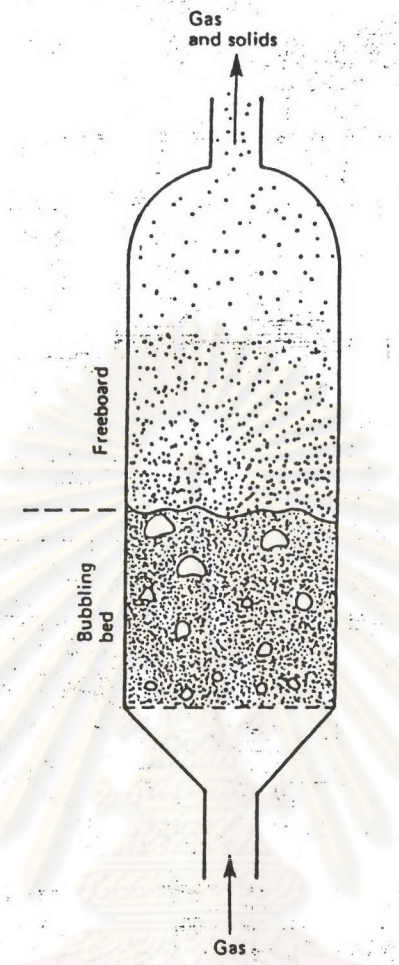

Figure 2.1 Schematic diagram of fluidized bed showing bubbling zone and freeboard zone

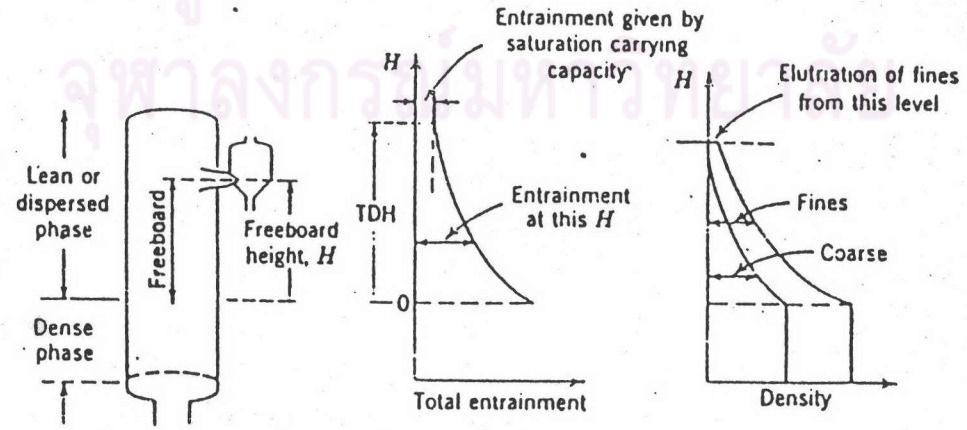

Figure 2.2 Schematic illustration of terms employed in the removal of solids from a bed

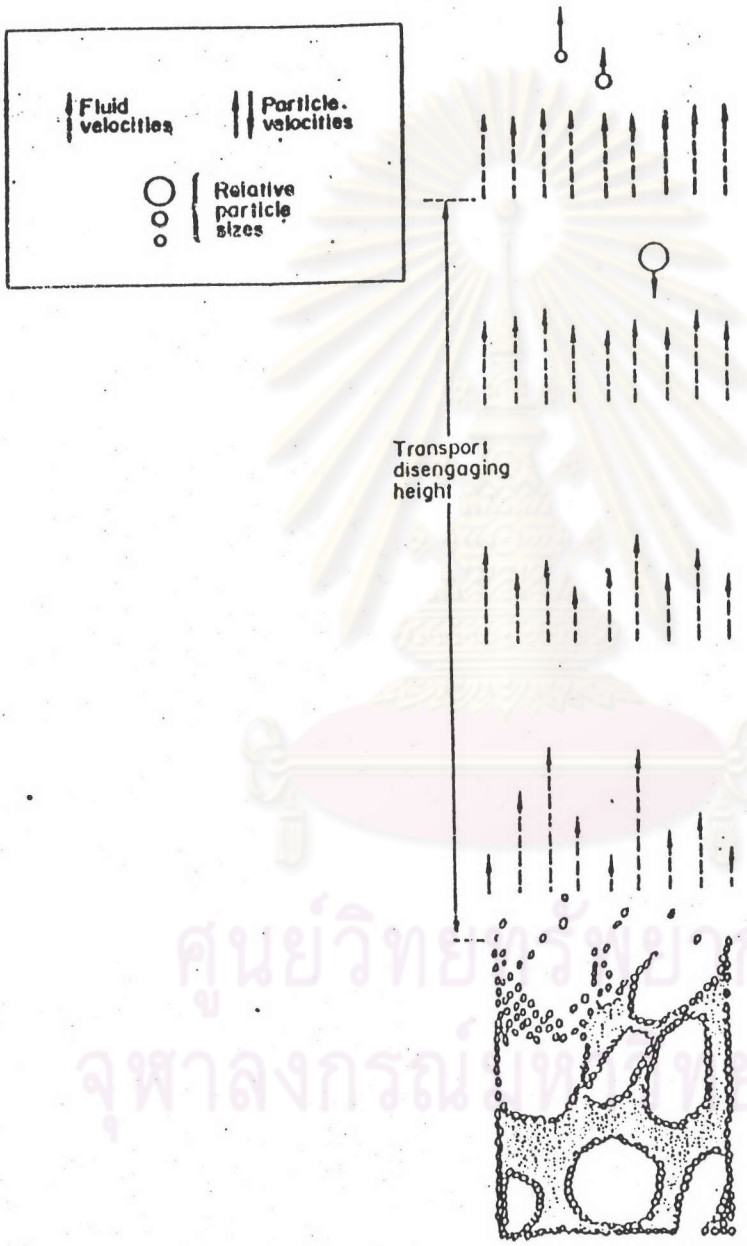

Figure 2.3 Upward and downward movement of particles according to their size in the freeboard zone

A thorough examination of freeboard phenomena suggested that particle separation could be done either by collection of particles at different levels in this zone, or by removing particles of desired size range provided the freeboard zone is designed to be high enough along together with controlled superficial velocity. Later case is the subject of interest in this investigation.

2.2 Entrainment and Elutriation

2.2.1 Early Development

The earliest quantitative correlation of elutriation above TDH was proposed by Leva (8), in 1951, who expressed the rate by a first order equation :

$$-\frac{dW_i}{dt} = kW_i \qquad (2.1)$$

where W_i is the weight of particle size i in the bed and k is the elutriation velocity constant.

In 1955, Yaki and Aochi (9) redefined the rate as

$$-\frac{1}{A_c}\frac{dW_i}{dt} = \frac{E_{i\infty}W_i}{W} \qquad (2.2)$$

where $E_{i\infty}$ is the elutriation rate constant and is independent of bed height. In comparison with equation 2.1, $E_{i\infty}$ is equal to kW/A_c. If the total weight of particle remaining in the bed, W, and bed cross-section area, A_c, were treated as constants, equation 2.2 may be expressed in term of mass fraction, X_i, as

$$-\left(\frac{W}{A_c}\right)\frac{dX_i}{dt} = E_{i\infty}X_i \qquad (2.3)$$

According to the authors, elutriation rate constant is independent of fine concentration up to 25 % based on the above equation.

The equation of Yaki and Aochi is widely accepted and many empirical correlations were reported for determining the elutriation rate constant, as seen

in Table 2.1. Dimensionless groups were used to relate $E_{i\infty}$ with system parameters, however, the application of these correlations are limited to the experimental conditions.

Correlation other than first order rate equation was also published by Thomas *et al.* (10), using the expression :

$$-\frac{dX_i}{dt} = c_1X_i(1 + c_2X_i) \qquad (2.4)$$

2.2.2 Kunii and Levenspiel's Model

In 1969, Kunii and Levenspiel (11) proposed an entrainment and elutriation model (Figure 2.4) based on the following assumptions :

1. The freeboard consists of three distinct phases, (a) gas stream with completely dispersed particles, these particles are transported pneumatically with velocity u_1, (b) projected agglomerates moving upward with velocity u_2 and (c) descending agglomerates and particles of thick dispersion moving downward with velocity u_3.

2. At any level in the bed the rate of dissipation of agglomerates to form dispersed solid of phase 1 is proportional to the concentration of agglomerate solid at that level.

3. Upward-movement agglomerates occasionally reverse direction and move downward, and the frequency of this change from phase 2 to phase 3 at any level is proportional to the solid concentration in phase 2 at that level.

By using mass balance on each phase and solving the equations with boundary conditions, the following correlation is obtained

$$\frac{1 - F/F_0}{1 - F_S/F_0} = 1 - e^{-aH} \qquad (2.5)$$

Table 2.1 Published correlations for calculation of elutriation rate constant

Yagi and Aochi (1955)

$$\frac{E_{t\infty}\, g\, d_p^2}{\mu\,(U_o - U_{ts})^2} = 0.0015\, \mathrm{Re}_t^{0.6} + 0.01\, \mathrm{Re}_t^{1.2}$$

Zenz and Weil (1958)

$$\frac{E_{t\infty}}{\rho_g\, U_o} = \begin{cases} 3.91 \times 10^2 \left(\dfrac{U_o^2}{g\, d_p\, \rho_s^2}\right)^{1.87}, & \dfrac{U_o^2}{g\, d_p\, \rho_s^2} \le 581.8 \times 10^{-3} \\ 7.02 \times 10^3 \left(\dfrac{U_o^2}{g\, d_p\, \rho_s^2}\right)^{1.15}, & \dfrac{U_o^2}{g\, d_p\, \rho_s^2} \ge 581.8 \times 10^{-3} \end{cases}$$

Wen and Hashinger (1960)

$$\frac{E_{t\infty}}{\rho_g\,(U_o - U_{ts})} = 1.52 \times 10^{-5} \left[\frac{(U_o - U_{ts})^2}{g\, d_p}\right]^{0.5} \mathrm{Re}_t^{0.725} \left(\frac{\rho_s - \rho_g}{\rho_g}\right)^{1.15}$$

Tanaka et al. (1972)

$$\frac{E_{t\infty}}{\rho_g\,(U_o - U_{ts})} = 4.6 \times 10^{-2} \left[\frac{(U_o - U_{ts})^2}{g\, d_p}\right]^{0.5} \mathrm{Re}_t^{0.3} \left(\frac{\rho_s - \rho_g}{\rho_g}\right)^{0.15}$$

Merrick and Highley (1974)

$$\frac{E_{t\infty}}{\rho_g\, U_o} = A + 130 \exp\left[-10.4 \left(\frac{U_{ts}}{U_o}\right)^{0.5} \left(\frac{U_{mf}}{U_o - U_{mf}}\right)^{0.25}\right]$$

Geldart et al. (1979)

$$\frac{E_{t\infty}}{\rho_e\, U_o} = 23.7 \cdot \exp\left(-5.4\, \frac{U_{ts}}{U_o}\right)$$

$\rho_e = \rho_g + \Sigma \rho_i$ (ρ_i: solid loading of ith size fraction in exit gas)

Colakyan et al. (1979)

$$E_{t\infty} = 33 \left(1 - \frac{U_{ts}}{U_o}\right)^2$$

Bachovchin et al. (1979)

$$E_{t\infty} = 3.35 \times 10^{-5} \left(\frac{U_o}{\sqrt{\bar{d}_p\, g}}\right)^{4.67} \left(\frac{\rho_g}{\rho_s}\right)^{1.62} \left(\frac{\mu}{\bar{d}_p}\right) \left(\frac{D_c \sqrt{X_s}}{\bar{d}_p}\right)^{1.15}$$

where

$\bar{d}_p$: average size of particle elutriated

X_s: fraction of fines at the bed surface

Lin et al. (1980)

$$\frac{E_{t\infty}}{\rho_g\, U_o} = 9.43 \times 10^{-4} \left(\frac{U_o^2}{g\, d_p}\right)^{1.65}$$

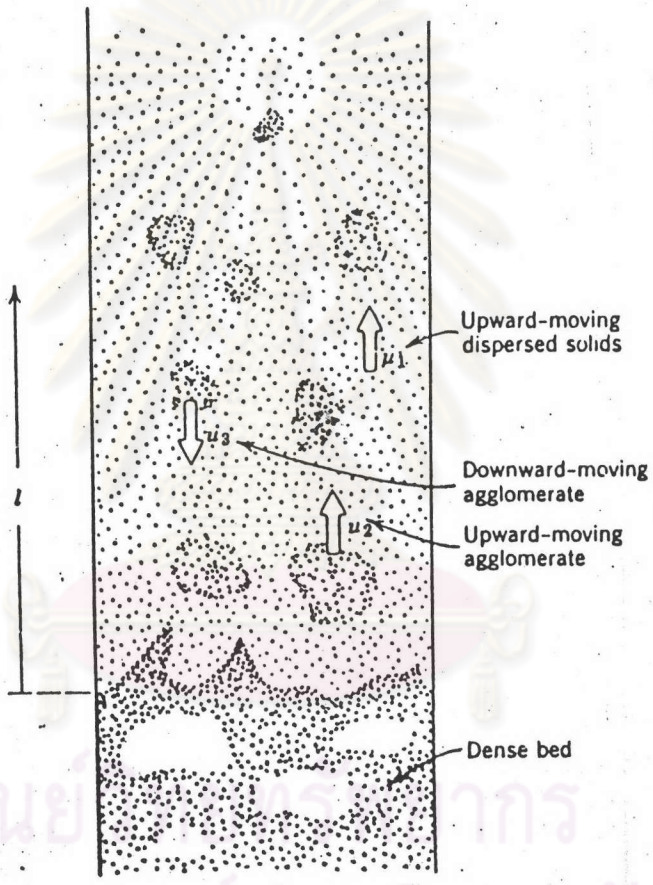

Figure 2.4 Schematic representation model for elutriation and entrainment from fluidized beds, according to Kunii and Levenspiel (11)

where

$$\frac{F_o}{F_o} = \frac{(1+ u_2/u_3)(K/K^*)}{1 + (1 + u_2/u_3)(K/K^*)}$$

$$a = \frac{K^*}{u_2}\left[1 - \left(1 + \frac{u_2}{u_3}\right)\frac{K}{K^*} \right]$$

K and K^* are rate coefficients, for transfer from phase 2 and phase 3 to phase 1, and for transfer from phase 2 to phase 3, respectively, F_o is the flow rate of solids projected from the bed surface, F_s is the mass flow rate corresponding to the saturation capacity of the flowing gas stream, and H is the freeboard height. Assuming that for normal entrainment conditions, much solid is projected from and returns to the bed, equation 2.5 was reduced to

$$F = F_o e^{-aH} \quad , \quad a = \frac{K^*}{u_2} \qquad (2.6)$$

Combining equations 2.6 and 2.2, will give the elutriation constant in terms of the model parameters.

$$E_{i\infty} = \frac{F_o}{A_c} e^{-aH} \quad , \quad a = \frac{K^*}{u_2} \qquad (2.7)$$

2.2.3 Wen and Chen's Model

Further development of model was carried out by Wen and Chen (12,13), following equation worked by Large *et al.* (14).

$$F_i = F_{ei} + (F_{oi} - F_{ei})\, e^{-aH} \qquad (2.8)$$

where F_i is the total elutriation rate of particle size i, a is constant ranging from 3.5-6.4 m^{-1}, practically value of 4.0 m^{-1} is used. H is height above fluidized bed.

The total entrainment rate at bed surface, F_{oi}, is determined from erupting bubble diameter at bed surface, D_b, and the excess gas velocity $U-U_{mf}$.

$$\frac{F_o}{A_c D_b} = 3.07 \times 10^{-9} \frac{\rho_g^{3.5}\, g^{0.5}}{\mu^{2.5}} (U - U_{mf})^{2.5} \qquad (2.9)$$

where U is the superficial gas velocity. Entrainment of particle size d_{pi} at bed surface, F_{oi}, can be approximated by equation similar to Henry's Law as

$$F_{oi} = F_o X_i \qquad (2.10)$$

D_b can be calculated from empirical equation of Mori and Wen (15) :

$$\frac{D_{bm} - D_b}{D_{bm} - D_{bo}} = \exp(-0.3h/D) \qquad (2.11)$$

where D is bed diameter, h is the height of fluidized bed surface measured from distributor plate. D_{bm} is the maximum bubble diameter due to total coalescences of bubbles and can be calculated from.

$$D_{bm} = 0.625 \left[A_c (U - U_{mf}) \right]^{2/5} \qquad (2.12)$$

D_{bo}, the initial bubble diameter formed at the surface of distributor plate, for perforated plate, could be calculated from

$$D_{bo} = 0.347 \left[\frac{A_c(U - U_{mf})}{N_d} \right]^{2/5} \qquad (2.13)$$

where N_d is total number of orifices on the plate.

Another correlation which Wen and Chen used for calculating D_b is equation of Cranfield and Geldart (16). It is not discussed here since in this study the flow regimes fall within the range of Mori and Wen work. The minimum fluidized velocity, U_{mf}, may be estimated from Wen and Yu equation (17), which could be applied for whole range of Reynolds number.

$$Re_{mf} = \left[(33.7)^2 + 0.0408\, G_a \right]^{1/2} - 33.7 \qquad (2.14)$$

where $$Re_{mf} = \frac{U_{mf} d_{pi} \rho_g}{\mu_g}$$

and $$G_a = \frac{d_{pi}^3 \rho_g (\rho_s - \rho_g) g}{\mu^2_g}$$

F_{ei} in equation 2.9 is the elutriation rate as in equation 2.3. Elutriation rate constant, $E_{i\infty}$, is calculated as follows:

$$E_{i\infty} = \rho_s (1 - \varepsilon_i)(U - U_t) \quad (2.15)$$

$$\varepsilon_i = \left[1 + \frac{\lambda (U - U_t)^2}{2gD} \right]^{-(1/4.7)} \quad (2.16)$$

$$\frac{\lambda \rho_s}{d_{pi}^2} \frac{\mu_g^{2.5}}{\rho_g^{2.5}} = \begin{cases} (5.17 Re_p^{-1.5} D^2 , Re_p \leq 2.38/D) \\ (12.3 Re_p^{-2.5} D , Re_p \geq 2.38/D) \end{cases} \quad (2.17)$$

here $$Re_p = \frac{\rho_g (U - U_t) d_{pi}}{\mu_g}$$

where ε_i is the voidage of fine particle in freeboard and λ is the friction coefficient due to the bouncing of the particle against wall and against each other. Postulation of these correlations is based on that when particles of a single size are elutriated above TDH, the saturation carrying capacity of the gas stream under pneumatic transport conditions is reached. The rate of elutriation from a bed composed of a single-sized particle can be viewed as independent of a hydrodynamics prevailing inside the bed (18).

The single-particle terminal velocity, U_t, can be determined (19) by Stokes' law

$$U_t = \frac{d_{pi}^2 (\rho_s - \rho_g) g}{18 \mu_g} , \quad Re < 0.4 \quad (2.18)$$

or Intermediate law .

$$U_t = \left[\frac{4 (\rho_s - \rho_g)^2 g^2}{225 \rho_g \mu_g} \right]^{1/3} d_{pi} , \quad 0.4 < Re < 500 \quad (2.19)$$

or Newton's law

$$U_t = \left[\frac{3.1 (\rho_s - \rho_g) g d_{pi}}{\rho_g} \right]^{1/2} , \quad 500 < Re < 200{,}000 \quad (2.20)$$

here $$Re = \frac{\rho_g (U - U_t) d_{pi}}{\mu_g}$$

Wen and Chen compared their model with a wide range of previously reported results and found that it was well-fitted with these data. They stated that data employed to correlate the elutriation rate constants are based primarily on experiments utilizing air at room temperature, yet the application of the correlation to other gases at different temperatures should be done very cautiously. The range of applicability should not exceed the following limits :

0.1	$< U <$	10	(m/s)
860	$< \rho_s <$	7850	(kg/m^3)
37	$< d_{pi} <$	3400	(μm)
1.64×10^{-1}	$< \rho_g <$	1.18	(kg/m^3)
1.75×10^{-5}	$< \mu_g <$	4.5×10^{-5}	(kg/m.s)
0.034	$< D <$	2.06	(m)

Furthermore, this model was based on the results of one-species bed (system of one-kind particles), and most of the experimental data used for this correlation were merely of two-component, i.e., coarse and fine particles. Operation dealing with particles of more than one species or multimodal in size, the results may not be the same unless interaction or static force between the different kinds of particles are absent.

Equation 2.8 can be simplified when applied to large particles since the elutriation rate above TDH, F_{ci}, is small when compared with the entrainment rate at bed surface, F_o. So F_{ci} can be neglected and the equation is reduced to

$$F_i = F_{io}e^{-aH} \qquad (2.21)$$

On the other hand, for small particles the entrainment rate is approximately equal to the elutriation rate above TDH, thus,

$$F_i = F_{ci} \qquad (2.22)$$

2.3 Multi-Size, One-Kind Powder Bed

In 1951, Osberg and Charlesworth (20) had suggested that elutriation curves bend when more than one size particles are being elutriated. In the study on batch operation of multi-size one-kind powder bed in 1968, Hanesian and Rankell (21) found that the elutriation curves deviated from linear relation on log-normal plot, as seen in Figure 2.5. They described the rate characteristics as

$$\frac{X_i}{X_{io}} = be^{-k_1 t} + (1+b)e^{-k_2 t} \qquad (2.23)$$

where k_1 and k_2 represent the elutriation rate constants contributed by coarser and finer particles, respectively. They stated that " the phenomena would result from the fact that fine particles contribute relatively more to the elutriation rate at the beginning of the process than do the coarser fractions. Thus as elutriation continues, the bed becomes depleted of the finer sizes and the elutriation then corresponds to that of coarse sizes"

2.4 Two-Kind Powder Bed

In 1979, Geldart *et al.* (22) reported that in the absence of fines a bed of coarse particles fluidized at gas velocity below the terminal falling velocity of particles showed no elutriation; but when fine particles were added continuously to the bed, the coarse particles were forced into the upper reaches of the column and out into the cyclones. This was attributed to particle-particle interactions in the freeboard rather than to changes within the bed itself, and thus equation of Wen and Chen could not apply in this case.

2.5 Transport Disengagement Height (TDH)

It is interesting to note that almost all works discussed above defined elutriation as the phenomenon occurring above TDH and entrainment rate of

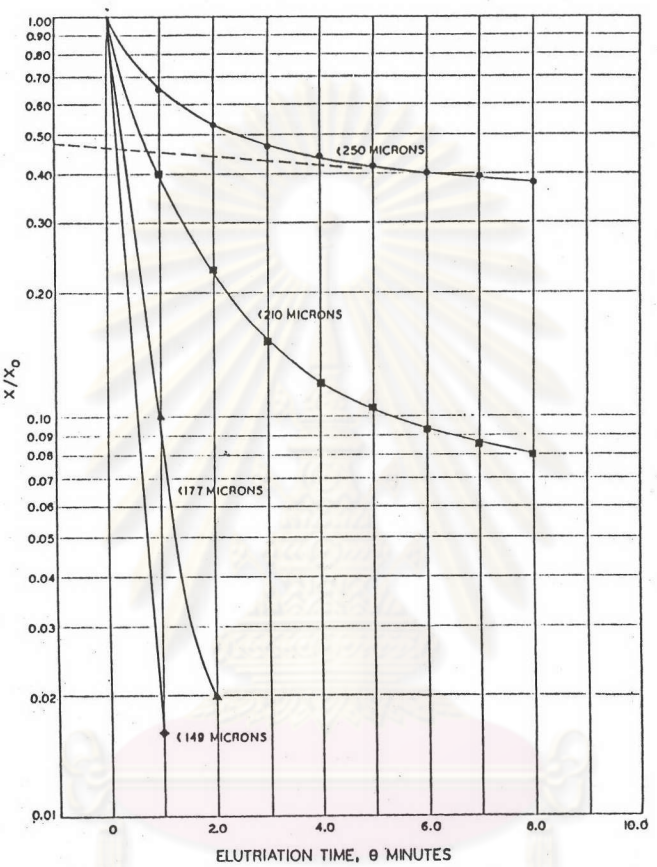

Figure 2.5 Characteristics of elutriation rate curve in multi-size one-kind powder bed (Hanesian and Rankell) (21)

particle decreases exponentially along the freeboard, under TDH boundary, however, a few studies were done in this area. Basically, TDH is directly related to particle size, diameter and superficial velocity. Zenz and Othmer (23) 1960, presented an empirical graphical correlation of TDH as shown in Figure 2.6, which is based primarily on fluid cracking catalyst particles. The authors also recommended it for particles up to 400 μm in diameter. Tanaka and Shinohara (24), 1978, suggested that one percent of the total amount of particle entrained at the bed surface be used for the calculation of TDH, i.e.

$$F\,(TDH) = 0.01F_o \qquad (2.24)$$

Wen and Chen (13) proposed method of estimation from equation 2.9 by assuming that the entrainment rate at the freeboard outlet is within a small percentage more than that of the amount of particle elutriated. For example, if the entrainment rate is within one more percent of elutriation rate, the freeboard height required is estimated to be

$$TDH = \left(\frac{1}{a}\right) \ln\left\{\frac{F_o - F_e}{0.01Fe}\right\} \qquad (2.25)$$

2.6 Fluidization Characteristics of Geldart's Group A powder

There are some powders differed from normal cases in that it is extremely difficult to fluidize. One of which is Geldart's Group A powder (19). Geldart classification was based on fluidization characteristics of the powder itself. This group of powder may be characterized by a relatively small particles size ($30<d_p>150$ μm) and a low particle density (<1500 kg/m^3), as shown in Figure 2.7. During initial state of fluidization, the gas is merely channeling all the way through the bed that remains practically static at all velocities up to the very

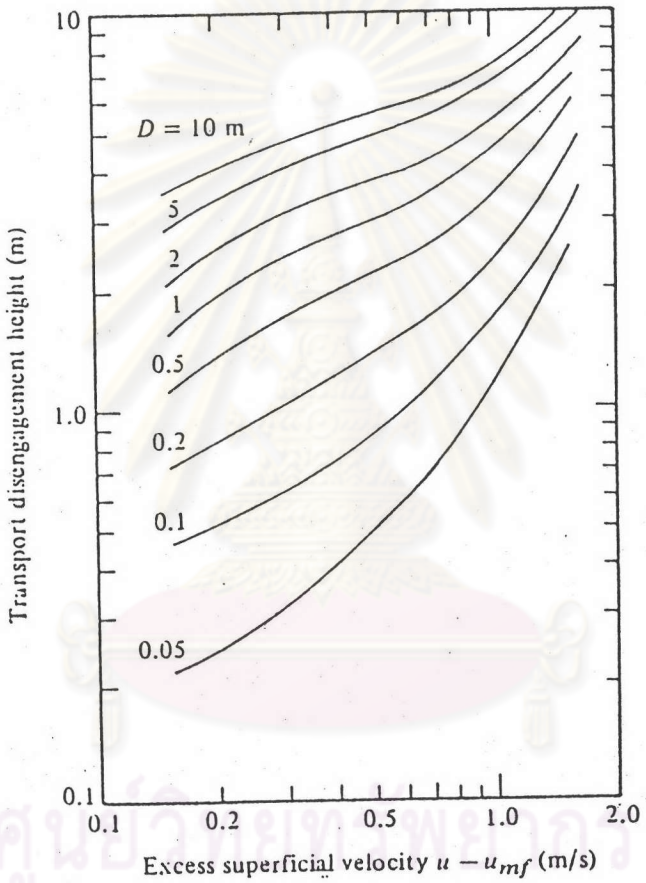

Figure 2.6 Simple graphic correlation based on Zenz & Weil (1958) and Zenz & Othmer (1960) for predicting TDH with fine solids

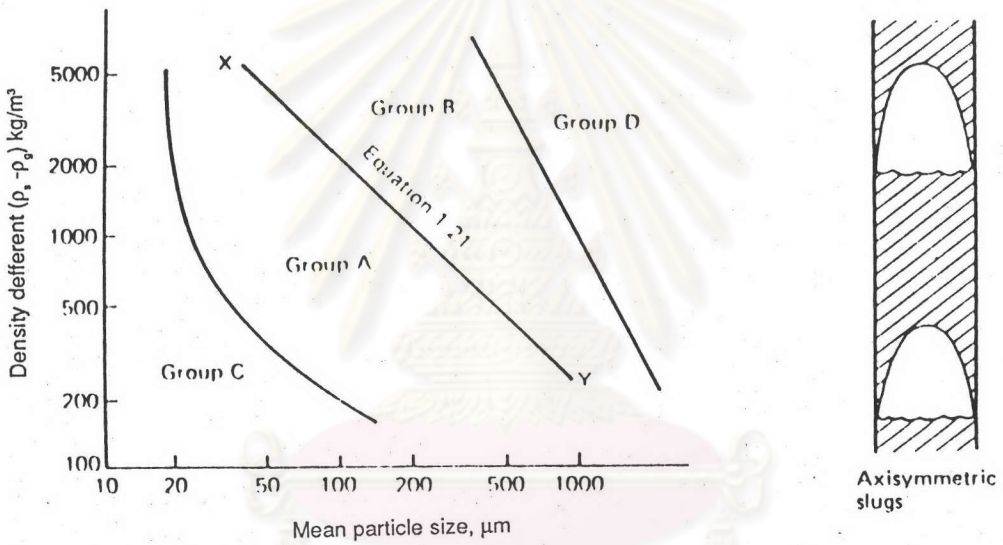

Figure 2.7 Powder classification diagram for fluidization by air (ambient condition) and characteristics of axisymmetric slug flow

highest. Frequently this group of powder shows an increase in void fraction of emulsion phase as the fluidizing gas velocity increases. The minimum bubbling velocity is always greater than the minimum fluidized velocity.

To estimate the U_{mf} of group A powder, it is suggested that the laminar part of Wen and Yu's equation is sufficient,

$$U_{mf} = \frac{9x10^{-4} (\rho_s - \rho_g)^{.934} g^{.934} d_{sm}^{1.8}}{\mu_g^{0.87} \rho_g^{0.066}} \qquad (2.26)$$

where d_{sm} is the surface mean diameter defined as

$$d_{sm} = \frac{1}{\sum \frac{X_i}{d_a}} \qquad (2.27)$$

here X_i is the mass fraction of particles in each size range given by sieve aperture, d_a. Furthermore, the axisymmetric slug flow is normally formed in the bed belonged to this group of powder, as seen in Figure 2.7.

Remark must be made here that there is a limited number of studies on systems containing more than one kind of particles as well as lack of reports on elutriation under TDH. In practice, it is possible to be handling with systems of multiple species and also the fluidized bed of column height lower than TDH.